



OUTLINE

- What's next after IMRT and VMAT ?

- Digital LINAC
- Beam level imaging & imaging of RT beams
- Station parameter optimized radiation therapy (SPORT)
- New QA tools for emerging RT technologies

ACKNOWLEDGEMENT

National Cancer Institute &
Varian Medical Systems

Ruijiang Li, Karl Bush, Benjamin
Fahimian, Dimitre Hristov, Victor Yu,
Bin Han, Gary Luxton



New Generation of Digital LINACs

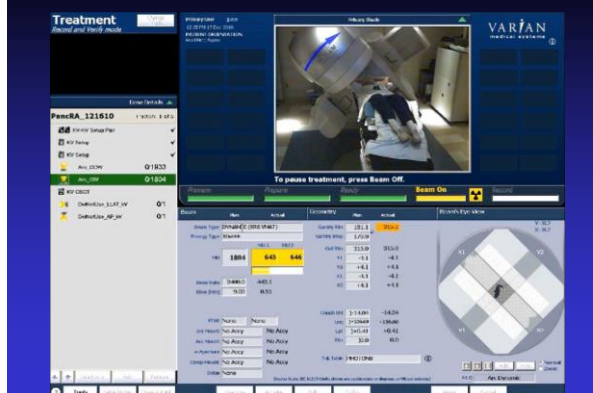
Versa - Elekta

TrueBeam™ STx at Stanford



One of the first three TrueBeam LINACs - installed in 2009,
Commissioning & acceptance test: July 2010, First SBRT
patient: Sept. 2010

Gated RapidArc Treatment Delivery

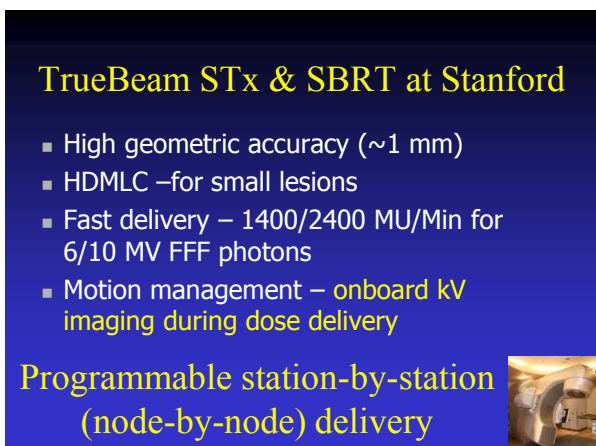
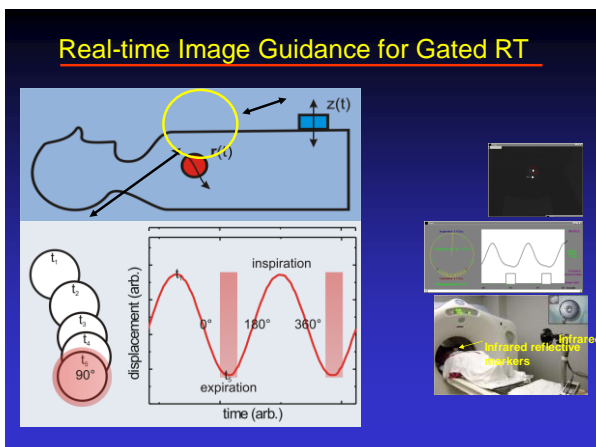
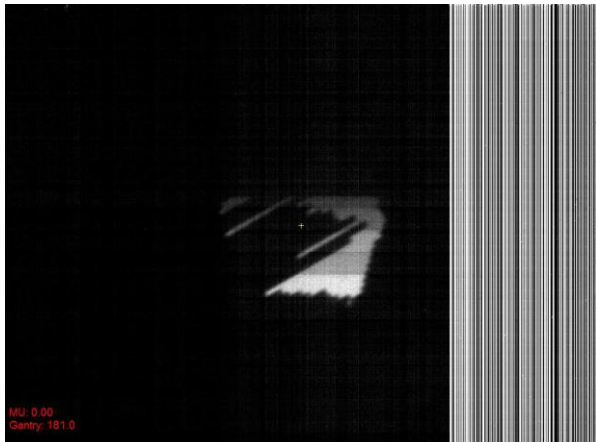


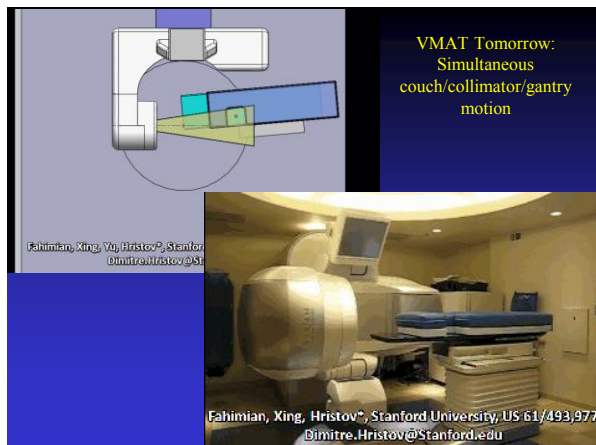
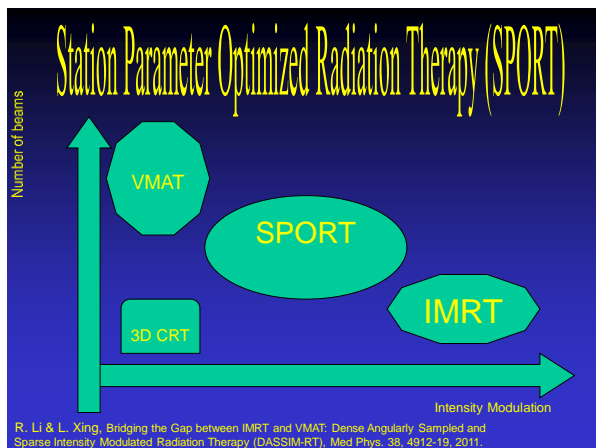
Beam-Level Imaging: Verification of Geometric Accuracy

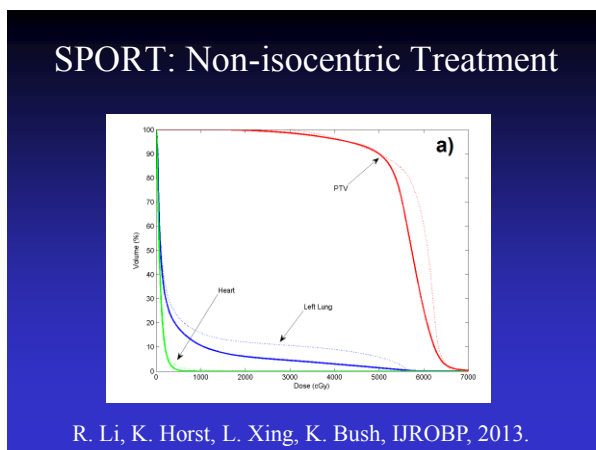
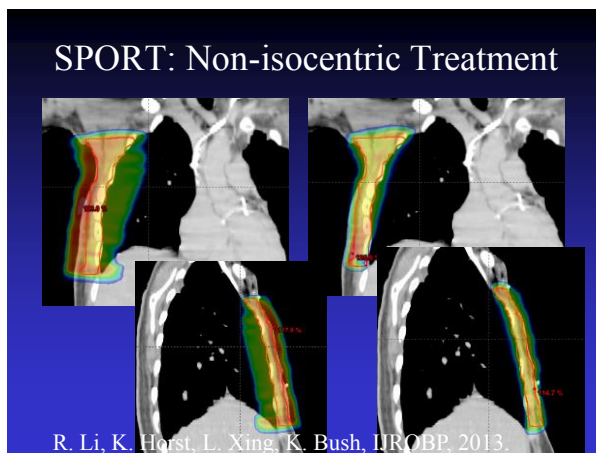
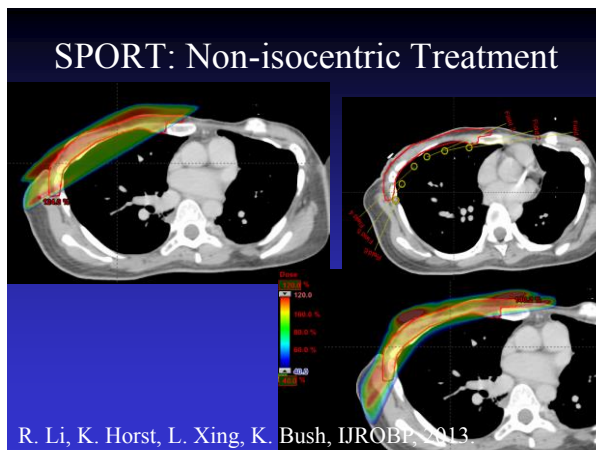
- During treatment, acquire kV images at the beginning of beam on for every breathing cycle.
- For each image,
 - Detect fiducials
 - Estimate 3D positions
 - Compare fiducials with software “markers”



Ruijiang Li et al, Stanford





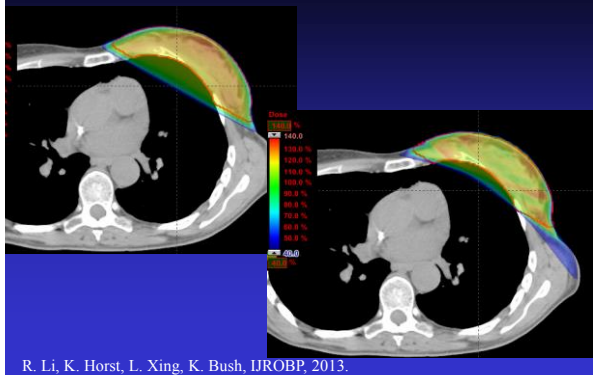


SPORT: Non-isocentric Treatment



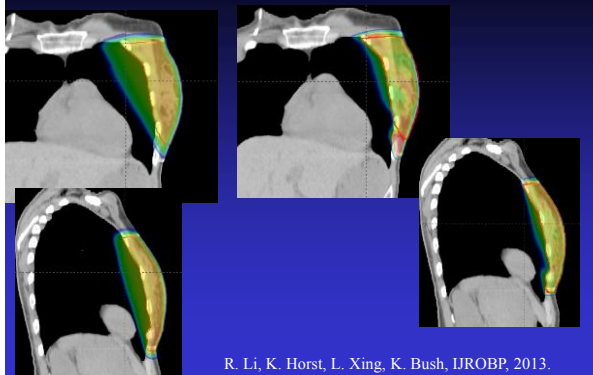
R. Li, K. Horst, L. Xing, K. Bush, IJROBP, 2013.

Non-isocentric Tx Bush and Li



R. Li, K. Horst, L. Xing, K. Bush, IJROBP, 2013.

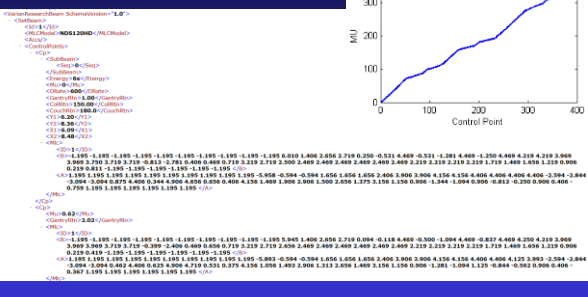
Non-isocentric Trreatment



R. Li, K. Horst, L. Xing, K. Bush, IJROBP, 2013.

TrueBeam developer mode

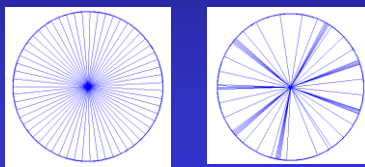
- Custom beam data in xml



SPORT implementations for replacing RapidArc:

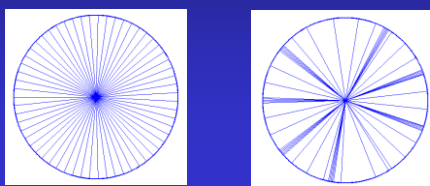
Method I: Segmentally boosted VMAT – adding a few segments in certain directions and optimize the RapidArc plan together with the added segments.

Improved dose distribution with a single arc.



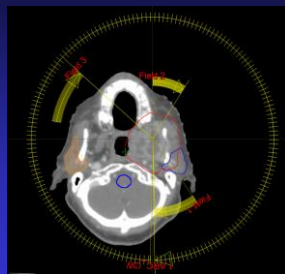
SPORT implementations for replacing RapidArc®

Method II: Differentially boosted VMAT – adding a few apertures to certain angular regions and optimize the system. An adaptive optimization algorithm has been developed for this purpose.

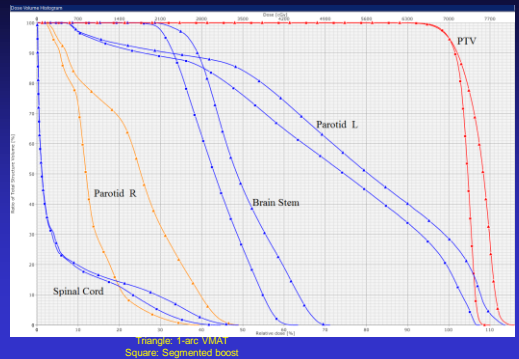


Field Setup

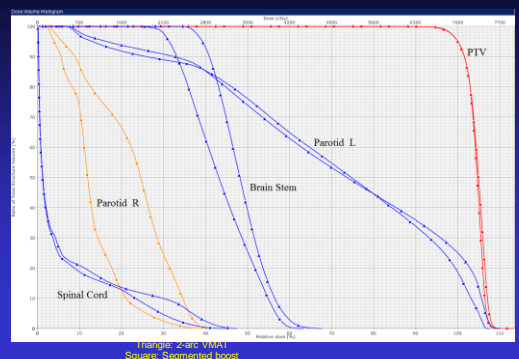
- Single full arc VMAT
- Boosted partial arcs
 - 3 arcs in this HN case
 - each ~30 deg
- Treatment planning
 - VMAT optimization



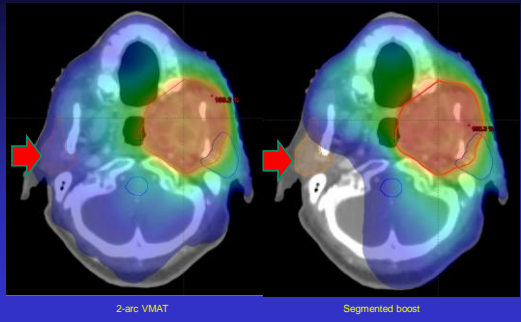
Comparison with single-arc



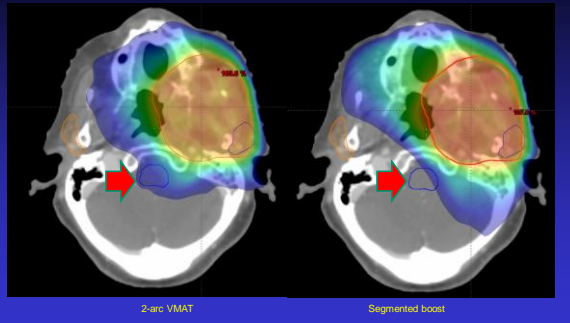
Comparison with double-arc VMAT



Iso-dose distributions (20% and above)

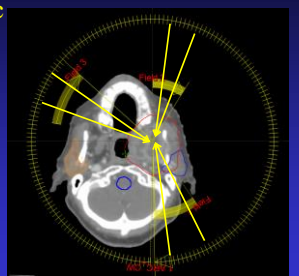


Iso-dose distributions (45% and above)



Treatment delivery

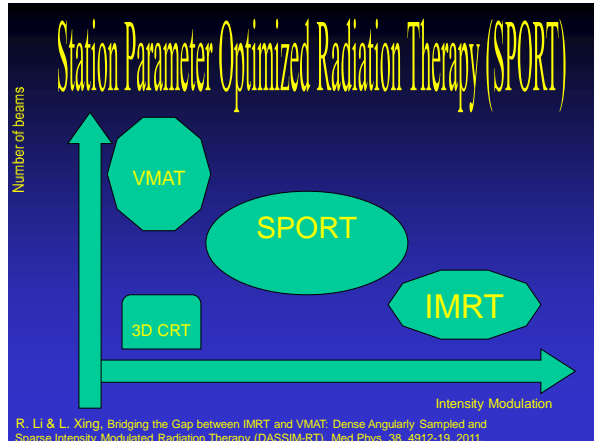
- Delivered in a single-arc
 - Each of the 3 partial arcs is converted into 2 static sub-fields.
 - 1 continuous arc with 6 static beams inserted



Delivery summary

- Rx: 200 cGy times 35 fractions

	MU	Control Points	Gantry span (deg)	Delivery time
1-ARC VMAT	276	178	360	1 min
2-ARC VMAT	520	376	720	2 min
Segmented boost	331	376	450	1 min 55 sec



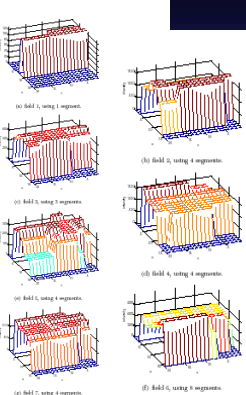
Search for IMRT inverse plans with piecewise constant fluence maps using compressed sensing techniques

Lei Zhu^a and Lei Xing^b

^aDepartment of Radiation Oncology, Stanford University, Stanford, California

(Received 3 October 2008; revised 5 February 2009; accepted for publication 27 April 2009)

An intensity-modulated radiation therapy (IMRT) field is composed of a set of beamlets that define the final dose distribution. In this article, the authors quantify the sparsity of the fluence map and propose a novel method to solve the inverse problem of IMRT using compressed sensing. A Pareto front is generated to achieve the tradeoff associated with the Pareto efficient point acceptance criteria. The clinically acceptable dose distribution weight is chosen as the final solution. The method is demonstrated in IMRT on a prostate patient. The result shows that the total number of beamlets can be reduced while maintaining a satisfactory dose distribution. With the focus on the sparsity of the fluence map, a new method is proposed to solve the inverse problem of IMRT using compressed sensing. © 2009 American Association of Physicists in Medicine.



Compressed Sensing-Based Inverse Planning Framework

minimize

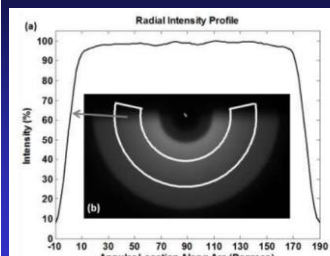
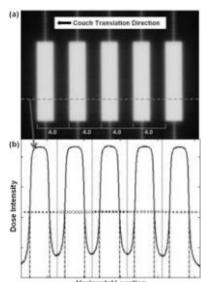
$$\begin{cases} \phi_1(x) = \sum_i \lambda_i (A_i x - d_i)^T (A_i x - d_i), \\ \phi_2(x) = \sum_{f=1}^{N_f} \sum_{u=2}^{N_u} \sum_{v=2}^{N_v} |\nabla_{u,v} x(u, v, f)| \end{cases}$$

subject to

$$x \succeq 0.$$

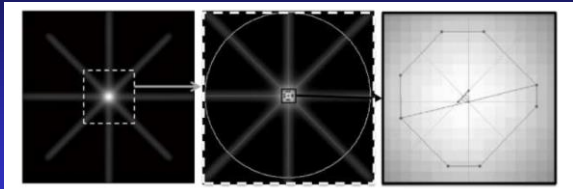
$$\nabla_{u,v} x(u, v) = |x_{u,v} - x_{u-1,v}| + |x_{u,v} - x_{u,v-1}|,$$

Quality Assurance of SPORT



V. Yu, B. Fahimian, L. Xing & D. Hristov, Med Phys, in press, 2014

Quality Assurance of SPORT



V. Yu, B. Fahimian, L. Xing & D. Hristov, Med Phys, in press, 2014

Quality Assurance of SPORT

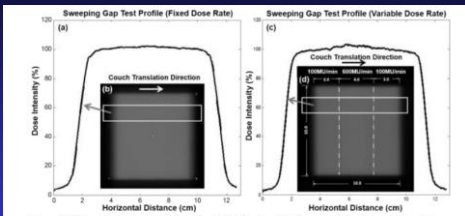
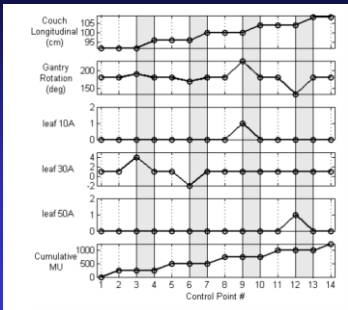


Figure 6. (a) Sweeping Gap Test (Fixed Dose Rate). Profile of relative dose intensity vs. horizontal location (cm). (b) Resultant film image with the indication of the location of the profile shown in (a). (c) Sweeping Gap Test (Variable Dose Rate). Profile of relative dose intensity vs. horizontal location (cm). (d) Resultant film image with the indication of the location of the profile shown in (c). To test dose rate variation, the test was delivered in three segments with maximum dose rates of 100, 600, and 100 MU/min, separations shown by the vertical dashed lines.

V. Yu., B. Fahimian, L. Xing & D. Hristov, Med Phys, in press, 2014

Quality Assurance of SPORT



V. Yu., B. Fahimian, L. Xing & D. Hristov, Med Phys, in press, 2014

Quality Assurance of SPORT

Table 2. "Tracking Test" Results						
	Left to fiducial ^a		Right to fiducial ^b		End to end ^c	
Couch Direction	mean	std	mean	std	mean	std
Lateral	1.950	0.020	2.047	0.015	3.997	0.006
Longitudinal	1.970	0.010	2.033	0.006	4.003	0.006

^aLeft to fiducial: distance from left beam edge to fiducial in cm.

^bRight to fiducial: distance from right beam edge to fiducial in cm.

^cEnd to end: size of beam along the translational axis in cm.

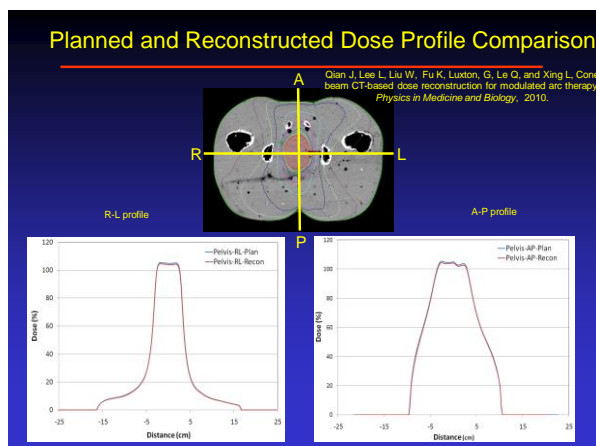
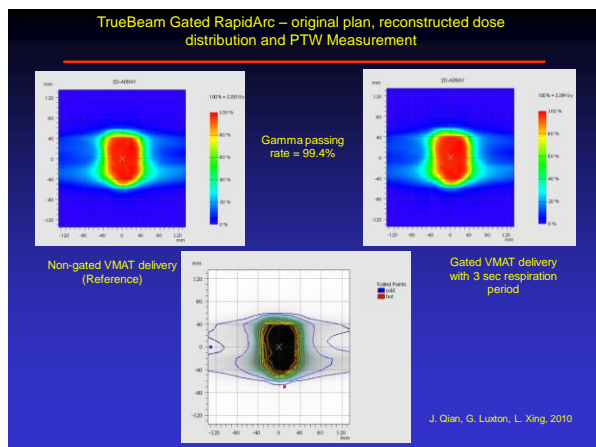
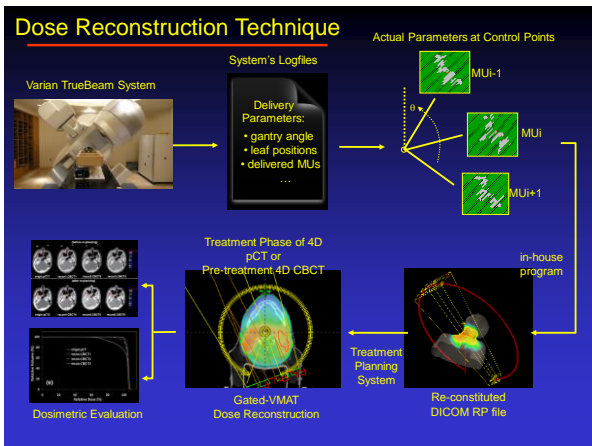
Table 1. "Sweeping Gap Test" Results.

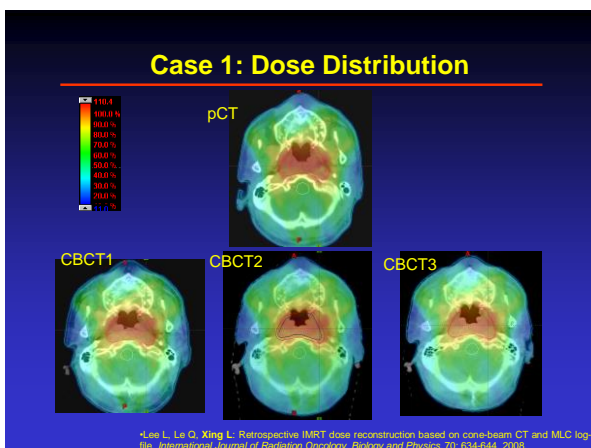
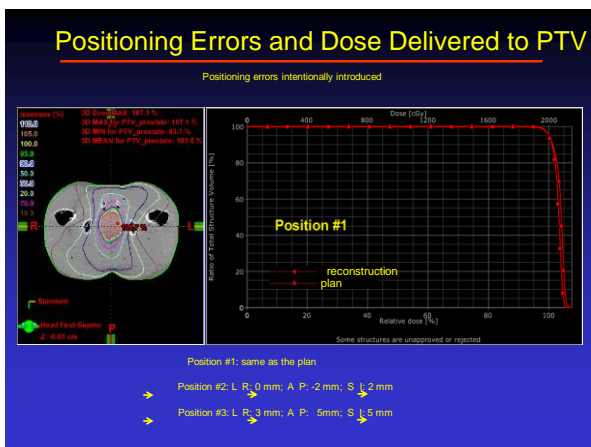
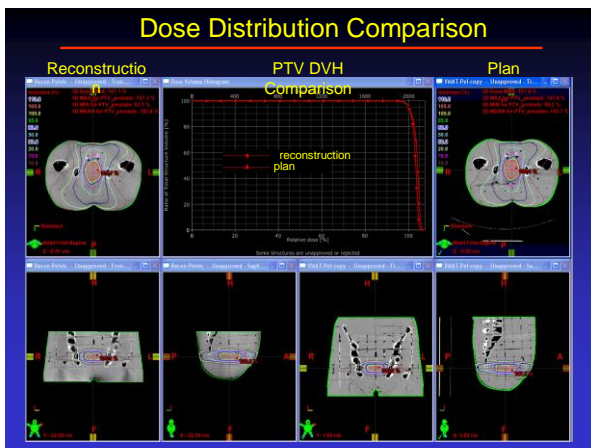
Deviations relative to mean in (%) for the case of fixed and variable dose rate during the delivery of the sweeping gap.

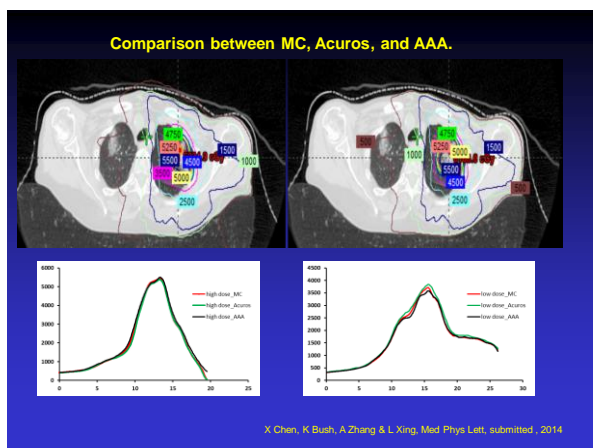
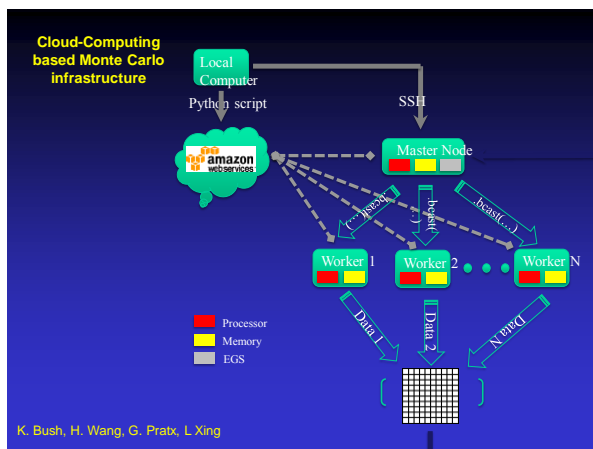
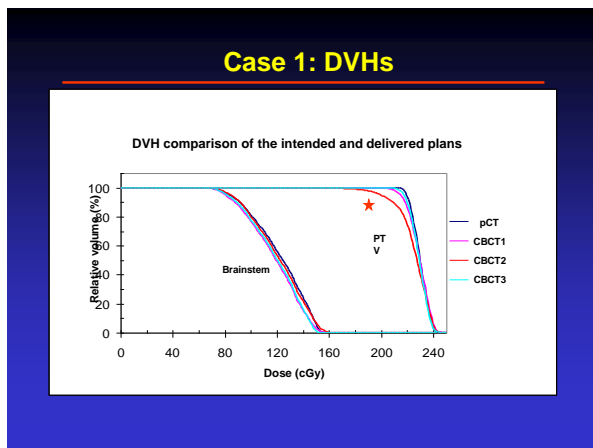
Deviation relative to the mean (Fixed Dose Rate) (%)

Couch movement direction	standard deviation	maximum deviation
Lateral	0.37	1.04
Longitudinal	0.52	1.10
Deviation relative to the mean (Variable Dose Rate) (%)		
Lateral	0.95	1.98
Longitudinal	1.12	2.42

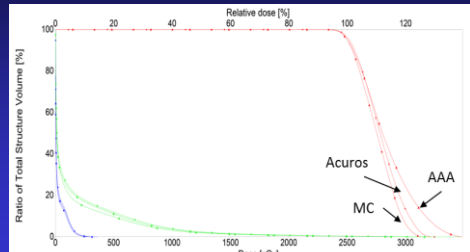
V. Yu., B. Fahimian, L. Xing & D. Hristov, Med Phys, in press, 2014



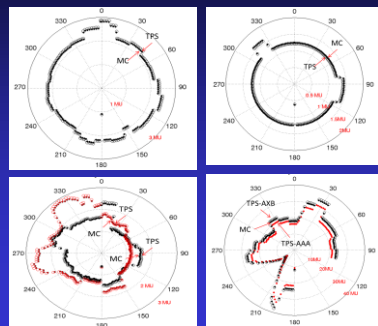




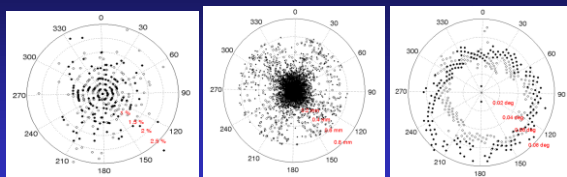
MU verification for VMAT



MU verification for VMAT



MU verification for VMAT



EPID-based absolute dosimetry for digital linac

- unflattened beam
- high dose rate
- small sized fields in (SBRT)

Routine SBRT QA

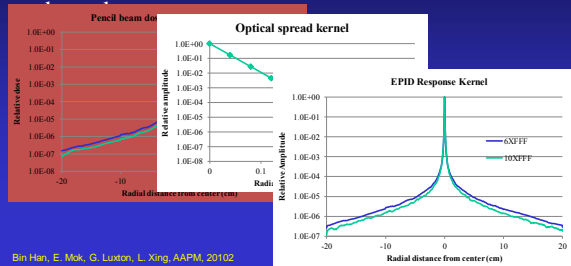
- High efficiency
- High dose resolution
- Ease of use



Bin Han, E. Mok, G. Luxton, L. Xing, ASTRO, 2013

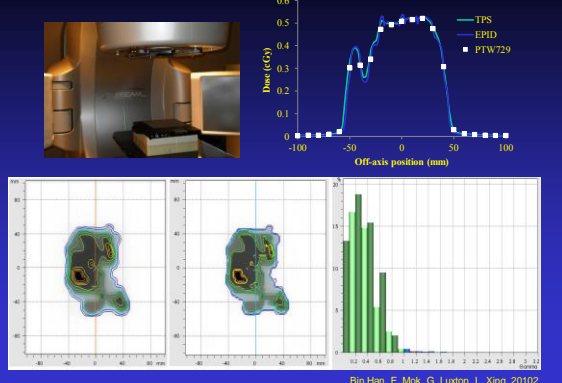
EPID Response Core

- Monte Carlo dose distribution kernel, Optical spread kernel, Total EPID response



Bin Han, E. Mok, G. Luxton, L. Xing, AAPM, 20102

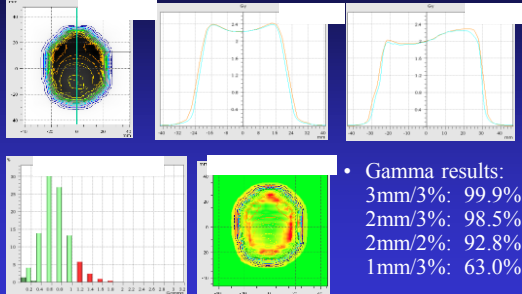
EPID-based absolute dosimetry



Bin Han, E. Mok, G. Luxton, L. Xing, 20102

Result: EPID dosimetry for SBRT pt QA

6XFFF EPID vs. TPS verification plan



SUMMARY

- Features available in new generation of LINACs facilitate RT workflow and improve the efficiency & accuracy.
- Mechanical accuracy & imaging.
- SPORT.
- New QA tools are urgently needed.